The regional estimates of the GPS satellite and receiver differential code biases

Saeed Farzaneh[1*] and Mohammad Ali Sharifi[2,3]

[1] Assistant Professor, Department of Surveying and Geomatics Engineering, University College of Engineering, University of Tehran, Tehran, Iran
[2] Associate Professor, Department of Surveying and Geomatics Engineering, University College of Engineering, University of Tehran, Tehran, Iran
[3] Research Institute of Geoinformation Technology (RIGT), College of Engineering, University of Tehran, Tehran, Iran

(Received: 29 December 2016, Accepted: 17 April 2017)

Abstract

The Differential Code Biases (DCB), which are also termed hardware delay biases, are the frequency-dependent time delays of the satellite and receiver. Possible sources of these delays are antennas and cables, as well as different filters used in receivers and satellites. These instrumental delays affect both code and carrier measurements. These biases for satellites and some IGS stations tend to be obtained from the Center for Orbit Determination in Europe (CODE) as daily or monthly constants, which are based on the global ionospheric total electron content (TEC) modeling in the solar-geomagnetic frame. These biases are not provided for regional and local network receivers, and need to be computed by the user. In this study, the regional approach by the spherical Slepian function was used to estimate the GPS satellite and receiver DCBs. Validations using real data showed that this method has significant potential and the ability to yield reliable results, even for a single station DCB estimate.

Keywords: DCB, GPS, Slepian function, regional modeling

[*]Corresponding author: farzaneh@ut.ac.ir

1 Introduction

Global Positioning System (GPS) networks pave the way for studying the dynamics and continuous variations in the ionosphere by the complementary ionospheric measurements which are usually obtained by different techniques such as ionosondes, incoherent scatter radars, and satellites. The free electrons in the ionosphere have a strong impact on the propagation of radio waves. When the signals pass through the ionosphere, both their group and phase velocities are disturbed. The resulting effect in the first approximation is proportional to Total Electron Content along the signal path and inversely proportional to the frequency squared. TEC is one of the physical parameters that can be derived from the GPS data, and supply a symptom of ionospheric variability. The modeling of the ionospheric TEC is a significant domain for the radio wave propagation, geodesy, surveying, understanding of space weather dynamics and error correction related to Global Navigation Satellite Systems (GNSS) utilizations.

The Differential Code Biases, also termed hardware delays (e.g. the satellite or receiver) result in the frequency-dependent biases on both pseudorange and carrier phase measurements. These biases are not accessible in the absolute sense. Rather, they tend to be determined in a relative manner, e.g. the linear geometry combination for ionosphere modeling (Dach et al., 2007). Since the magnitude of the combined satellite and receiver DCBs can reach up to several nanoseconds (ns), this bias seriously affects the accuracy of certain applications, such as ionospheric TEC estimation (Conte et al., 2011; Wen et al., 2010; Ciraolo et al., 2007; Komjathy et al., 2005; Yuan and Ou, 1999; Mannucci et al., 1999; Lanyi and Roth, 1988; Wilson and Mannucci, 1993; Coco et al., 1991), and time transfer (Ray and Senior, 2005; Wilson et al., 1999).

The International GNSS Service (IGS) Analysis Centers calculate the satellite and the receiver differential code biases using the data network of the international GPS reference stations uniformly located in the world, which can be downloaded from the Center for Orbit Determination in Europe. These data are suitable for modeling the global ionospheric vertical total electron content and are not particularly suitable for regional modeling.

Many studies have been introduced to separate DCBs from TEC. Their methods can fall into two categories, namely the least-squares-based and non-least-squares-based methods. The former is based on estimating both the ionospheric models coefficients and DCBs from GPS dual frequency observations by the least-squares method (Durmaz and Karslioglu, 2014; Jin et al., 2012; Jin et al., 2008; Chen et al., 2004; Kee and Yun, 2002; Otsuka et al., 2002; Lin, 2001; Lanyi and Roth, 1988; Jakowski et al., 1996; Coco et al., 1991). The latter is based on searching for the true value with constraints through minimizing the standard deviation (Arikan et al., 2008; Ma and Maruyama, 2003; Zhang et al., 2003), which needs a large amount of computation, as well as an a priori search range. The selection of the search range is a critical parameter in this method. Should the search range be too broad, the computation will be time-consuming. Should the search range be too narrow, the true DCB value might not fall into this range, which could result in a wrong DCB estimate. In this work, we have proposed a new method for the regional modeling of VTEC, together with the satellite and receiver DCBs based on the weighted least-square method. The performance of the proposed method is tested with real data based on the five ground-based GPS observations which belong to the IGS networks for three days with different geomagnetic conditions.

2 Method of GPS DCB estimate

The satellite and receiver biases can seriously affect ionospheric TEC estimation. Therefore, it is necessary to precisely estimate GPS satellite and receiver DCBs to improve the accuracy of TEC estimates. The ionospheric delay in the GPS signals observed by ground stations can be converted into TEC, which is the total number of electrons in a column of the unit cross-section between the satellite and the receiver on the ground. The mathematical representation of the definition is (Liu and Gao, 2003):

$$\mathrm{STEC} = \int_{\mathrm{R}}^{\mathrm{S}} \mathrm{N_e}(\mathrm{r}, \theta, \lambda, \mathrm{t})\, \mathrm{dr}\,, \tag{1}$$

where N_e is the electron density at the time t, dr is the geometric range along the signal path between the satellite and the receiver, θ and λ are longitude and latitude and r is the signal path ray respectively. The ionospheric range delay I_i for the signal frequency f (Hz) can be written with respect to TEC as follows (Seeber, 2003):

$$\mathrm{I_i} = \pm \frac{40.3}{\mathrm{f}^2} \times \mathrm{STEC}\,. \tag{2}$$

Since the geometric range cannot be measured directly, TEC cannot directly be calculated from Equation (2) and therefore a method of measuring TEC directly from the differential code delay and carrier phase measurement on both the L1 and L2 frequencies is used. For this purpose, the geometry-free linear combination of pseudo range and carrier phase measurements (also termed ionospheric observable) is used as follows (Ciraolo et al., 2007):

$$\begin{aligned} \mathrm{P}_{4,\mathrm{r}}^{\mathrm{s}} &= \mathrm{P}_{1,\mathrm{r}}^{\mathrm{s}} - \mathrm{P}_{2,\mathrm{r}}^{\mathrm{r}} \\ &= \mathrm{I}_{1,\mathrm{r}}^{\mathrm{s}} - \mathrm{I}_{2,\mathrm{r}}^{\mathrm{s}} + \mathrm{br} + \mathrm{bs} + \varepsilon_{\mathrm{p}}\,, \end{aligned} \tag{3}$$

$$\begin{aligned} \Phi_{4,\mathrm{r}}^{\mathrm{s}} &= \Phi_{1,\mathrm{r}}^{\mathrm{s}} - \Phi_{2,\mathrm{r}}^{\mathrm{s}} \\ &= \mathrm{I}_{2,\mathrm{r}}^{\mathrm{s}} - \mathrm{I}_{1,\mathrm{r}}^{\mathrm{s}} + \lambda_1 \mathrm{N}_1 \\ &\quad - \lambda_2 \mathrm{N}_2 + \mathrm{Br} + \mathrm{Bs} + \varepsilon_{\mathrm{L}}\,, \end{aligned} \tag{4}$$

where $P_{1,r}^{s}, P_{2,r}^{s}, \Phi_{1,r}^{s}$ and $\Phi_{2,r}^{s}$ are the code and carrier phase pseudo ranges on the L1 and L2 signals, respectively. $I_{1,r}^{s}$ and $I_{2,r}^{s}$ are the ionospheric refraction delays at L1 and L2, respectively. $br = c(\tau_{p1}^{r} - \tau_{p2}^{r})$ and $Br = c(T_{L1}^{r} - T_{L2}^{r})$ are the code and phase inter-frequency biases (IFBs) for the receiver, $bs = c(\tau_{p1}^{s} - \tau_{p2}^{s})$ and $Bs = c(T_{L1}^{s} - T_{L2}^{s})$ are the code and phase differential inter-frequency biases for the satellite, ε_p and ε_L are the effects of multipath and measurement noise on the pseudo-range and carrier phase, respectively, λ_i is the wavelength of the L_i carrier phase, and N_i is the integer carrier phase ambiguity.

Since the noise level of the pseudorange GPS observations is relatively high and the ambiguity resolution is required for carrier phase observations, phase-smoothed code GPS observations are preferred to use for ionosphere modeling (Ciraolo et al., 2007; Nohutcu et al., 2010). By combining Equations (3) and (4) for simultaneous observations, the following equation can be obtained:

$$\begin{aligned} \mathrm{P}_4 + \Phi_4 &= \lambda_1 \mathrm{N}_1 - \lambda_2 \mathrm{N}_2 + \mathrm{Br} \\ &\quad + \mathrm{Bs} + \mathrm{br} + \mathrm{bs} + \varepsilon_{\mathrm{p}}\,. \end{aligned} \tag{5}$$

Due to the noise and multipath term for the carrier-phase observation is much lower than that for the pseudo-range observation, it can be neglected. The interval at which no cycle-slip error has occurred (leading to a constant phase ambiguity) is regarded as the continuous observational arc. For cycle slip detection, several testing quantities have been proposed based on various combinations of GPS observations (Seeber, 2003; or Hofmann-Wellenhof et al., 2008). Herein, observation file of each station has been processed individually and a single receiver test, i.e. the combination of a phase and a code range is applied for cycle slip detection (Hofmann-Wellenhof et al., 2008). The average values of the geometry-free pseudo-range and carrier phase is computed for any satellite and receiver in the continuous arc (Gao et al. 1994):

$$\begin{aligned}\left\langle \mathrm{P}_4 + \Phi_4 \right\rangle_{\mathrm{arc}} &= \frac{1}{\mathrm{n}} \sum_{\mathrm{i}=1}^{\mathrm{n}} (\mathrm{P}_4 + \Phi_4)_{\mathrm{i}} \\ &= \left\langle \lambda_1 \mathrm{N}_1 - \lambda_2 \mathrm{N}_2 \right\rangle_{\mathrm{arc}} + \mathrm{Br} \\ &\quad + \mathrm{Bs} + \mathrm{br} + \mathrm{bs} + \left\langle \varepsilon_{\mathrm{p}} \right\rangle_{\mathrm{arc}},\end{aligned} \tag{6}$$

where n is the number of measurements in the continuous arc. By subtracting Equation (6) from Equation (4) the ambiguity term is removed:

$$\begin{aligned}\tilde{\mathrm{P}}_4 &= \left\langle \mathrm{P}_4 + \Phi_4 \right\rangle_{\mathrm{arc}} - \Phi_4 \\ &\approx \mathrm{I}_1 - \mathrm{I}_2 + \mathrm{br} + \mathrm{bs} \\ &\quad + \left\langle \varepsilon_{\mathrm{p}} \right\rangle_{\mathrm{arc}} - \varepsilon_{\mathrm{L}}.\end{aligned} \tag{7}$$

where $\tilde{P}_4$ is the pseudo-range ionospheric observable smoothed by the carrier-phase ionospheric one. It will minimize the effect of multipath error so it can be neglected (Nohutcu et al., 2010). In order to extract STEC from the smoothed ionospheric observable, the ionospheric delays from Equation (2) are substituted into Equation (7):

$$\begin{aligned}\tilde{\mathrm{P}}_4 &= \mathrm{STEC} \times 40.3 \times \left(\frac{\mathrm{f}_2^2 - \mathrm{f}_1^2}{\mathrm{f}_1^2 \times \mathrm{f}_2^2} \right) \\ &\quad + \mathrm{br} + \mathrm{bs} + \left\langle \varepsilon_{\mathrm{p}} \right\rangle_{\mathrm{arc}} - \varepsilon_{\mathrm{L}}.\end{aligned} \tag{8}$$

Finally, STEC can be obtained in TECU ($\mathrm{TECU} = 10^{16} \mathrm{el\,m^{-2}}$):

$$\begin{aligned}\mathrm{STEC} &= (\tilde{\mathrm{P}}_4 - \mathrm{br} - \mathrm{bs} - \left\langle \varepsilon_{\mathrm{p}} \right\rangle_{\mathrm{arc}} + \varepsilon_{\mathrm{L}}) \\ &\quad \times \left(\frac{\mathrm{f}_1^2 \times \mathrm{f}_2^2}{40.3 \times (\mathrm{f}_2^2 - \mathrm{f}_1^2)} \right).\end{aligned} \tag{9}$$

Since in this study, the ionosphere is modeled as a thin single spherical layer, the STEC values have to be converted into the height-independent VTEC by introducing a mapping function (MF) (Schaer, 1999):

$$\begin{aligned}&\mathrm{MF} = \frac{\mathrm{STEC}}{\mathrm{VTEC}} = \frac{1}{\cos \mathrm{z}'}, \text{ with} \\ &\sin \mathrm{z}' = \frac{\mathrm{R_E}}{\mathrm{R_E} + \mathrm{H}} \sin \mathrm{z}\end{aligned} \tag{10}$$

where R_E is the mean Earth radius, z and z' are the zenith angles of the satellite at the user position and the ionospheric pierce point and H is the mean altitude which approximately corresponds to the altitude of the maximum electron density and its height can vary between 250 and 500 km depending on latitude, season, solar and geomagnetic activity conditions (Misra and Enge, 2003; Seeber, 2003; Schaer, 1999; Hofmann-Wellenhof et al., 2008).

In this research, the Slepian function was applied for the regional satellite and receiver DCBs estimation. The Slepian functions can be used effectively in the ionospheric application for TEC modeling (Sharifi and Farzaneh, 2013, 2015). These methods are used to find a set of band-limited functions with the optimal spatial concentration and space-limited functions with the minimal spectral leakage outside the bandwidth. These functions can be used as windows for the spectral analysis or as a sparse basis to represent and analyze the geophysical observables on a sphere. The necessary formula and more details can be extracted from Sharifi and Farzaneh (2013). In this approach the VTEC has to be represented as a function of the geomagnetic latitude β and the sun-fixed longitude s for a specified time interval $[t_{\min}, t_{\max}]$ (Schaer et al., 1995; Wielgosz et al., 2003):

$$\begin{aligned} \mathrm{TEC}(\beta,\mathrm{s}) &= \sum_{l=0}^{L}\sum_{m=-l}^{l} \omega_{lm} Y_{lm}(\beta,\mathrm{s}) \\ &= \sum_{n=1}^{(L+1)^2} \omega_n g_n(\beta,\mathrm{s}) \approx \sum_{n=1}^{N} \omega_n g_n(\beta,\mathrm{s}), \end{aligned} \tag{11}$$

where $Y_{lm}(\beta,s), g_n(\beta,s)$, ω, L and N are the spherical harmonic, spherical Slepian function, unknown coefficient, the bandwidth of the localization and Shannon number (the number of eigenfunctions optimally-concentrated within the region), respectively. The aforementioned VTEC modeling has been performed assuming that the ionosphere is static during the modeling period by neglecting the relatively small temporal variations in the ionosphere as a function of the geomagnetic latitude β calculated by:

$$\begin{aligned} \sin\beta &= \sin\varphi_g \sin\varphi_0 \\ &+ \cos\varphi_g \cos\varphi_0 \cos(\lambda_g - \lambda_0), \end{aligned} \tag{12}$$

where φ_0 and λ_0 are the geographical coordinates of the geomagnetic pole and (φ_g, λ_g) is the geographical coordinate of the station , and the sun-fixed longitude s (Schaer et al., 1995; Wielgosz et al., 2003):

$$\begin{aligned} \mathrm{S} &= \lambda_g + \mathrm{UT} - \pi \\ &= \lambda_g + (\mathrm{UT} - 12)^{\mathrm{hours}}, \end{aligned} \tag{13}$$

where s is in degree and UT is the universal time in hour. By substituting Equations (9) and (10) into Equation (11), the following expression can be obtained:

$$\begin{aligned} \sum_{n=1}^{N} \omega_n g_n(\beta,\mathrm{s}) &= \cos(\arcsin(\frac{R}{R+H}\sin(z)) \\ &\times \left[(\tilde{P}_4 - br_j - bs^i) \times \left(\frac{f_1^2 \times f_2^2}{40.3 \times (f_2^2 - f_1^2)} \right) \right], \end{aligned} \tag{14}$$

where ω_n, br_j and bs^i are the unknown parameters to be estimated. This equation is a final and fundamental formula for estimation of the unknown values. In this study a set of ionospheric coefficients was estimated every 1 hour. Since Equation (14) is singular (the satellite and receiver DCBs are linearly dependent), one exterior constraint must be added in order to separate the DCBs of the satellites and receivers. A general method is to force a mean zero constraint on the satellite DCBs (Schaer, 1999). Under this condition, Equation (14) reaches full rank and the DCBs of the satellites and receivers can be separated (Durmaz and Karslioglu, 2014; Jin et al., 2012).

3 Results and discussion

The regional DCB estimation in this study was based on the ground-based GPS observations collected across the Onsa, Pots, Gopi, Gras and Tehn stations, which belong to IGS network. The 24 h observations were obtained through the Internet and the sampling rate of the measurements was 30 s. The distribution of the stations has been illustrated in Figure 1. The STEC values for each observation were computed as described in Section 2. The altitude for the single layer model was set to 428.8 km for the calculation of VTEC and the elevation cut-off angle of 10° was used. The precise orbit files, provided by several IGS agencies, were interpolated to determine the satellite positions. These TEC measurements contain the ionospheric electron density information about the region above the GPS network and are used as the input data for the satellite and receiver DCBs estimation.

To demonstrate the performance of the proposed technique, the model was validated under different quiet and challenging ionospheric conditions, at different stations (in different latitudes and longitudes) and in different seasons. This evaluation contributed to taking into consideration solar cycle, seasonal, diurnal and latitude-dependent variations in this paper. To conduct the analysis, certain times were specified. This time interval was selected in order to model the VTEC distribution, which is strongly influenced by the aforementioned variations. Figure 2 shows the geomagnetic conditions for the evaluated days.

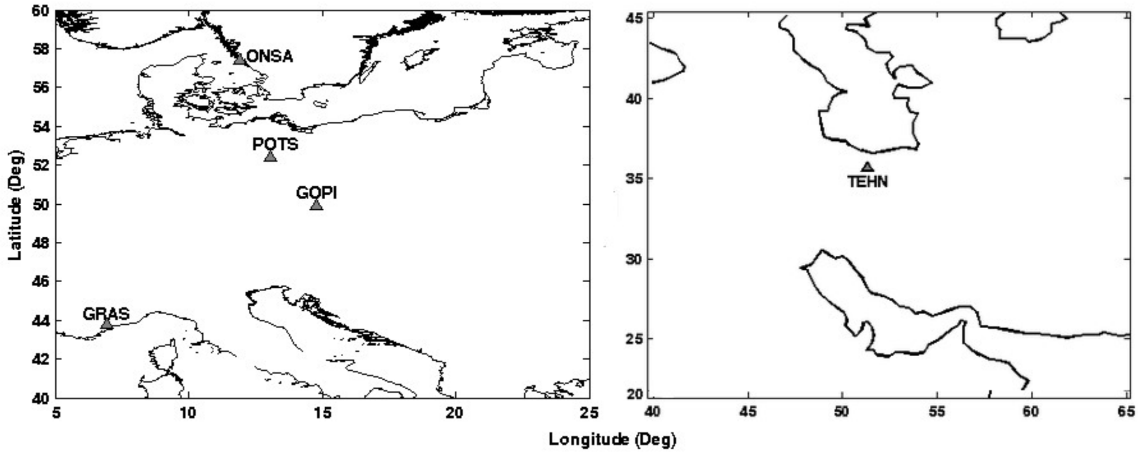

Figure 1. Distribution of the GPS stations.

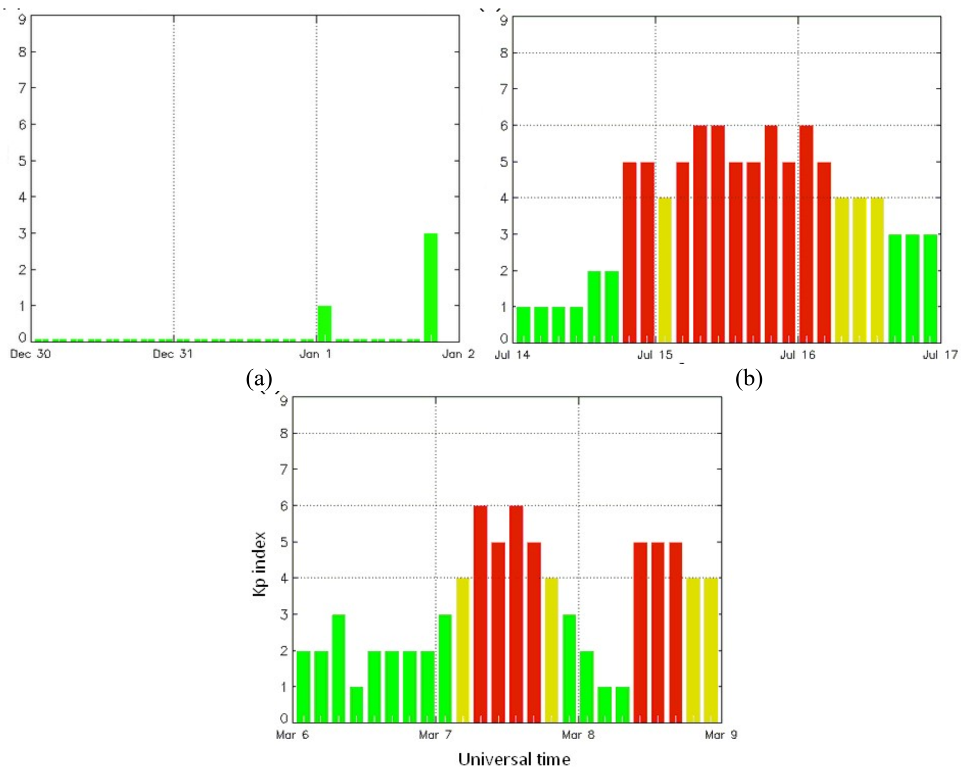

(a) (b) (c)

Figure 2. The estimated planetary K index for (a) Year 2010 Day Number 1, (b) Year 2012 Day Number 197, (c) Year 2012 Day Number 67 (http://www.spaceweatherlive.com).

The accuracy assessment was made in several ways. First, the proposed method was compared with the DCB estimates derived from the IGS analysis center products (CODE, ESA, JPL and IGS combined ionosphere maps). Figures 3 and 4 show the comparison of the estimated satellite and receiver DCBs, respectively, with those estimated by the CODE, ESA, JPL and IGS combined ionosphere maps. According to the figures, the differences between the IGS centers product and the proposed method are less than 1 ns for most of the satellites and receivers. These results indicate that the proposed method delivers stable receiver and satellite DCB estimates for the given days and stations.

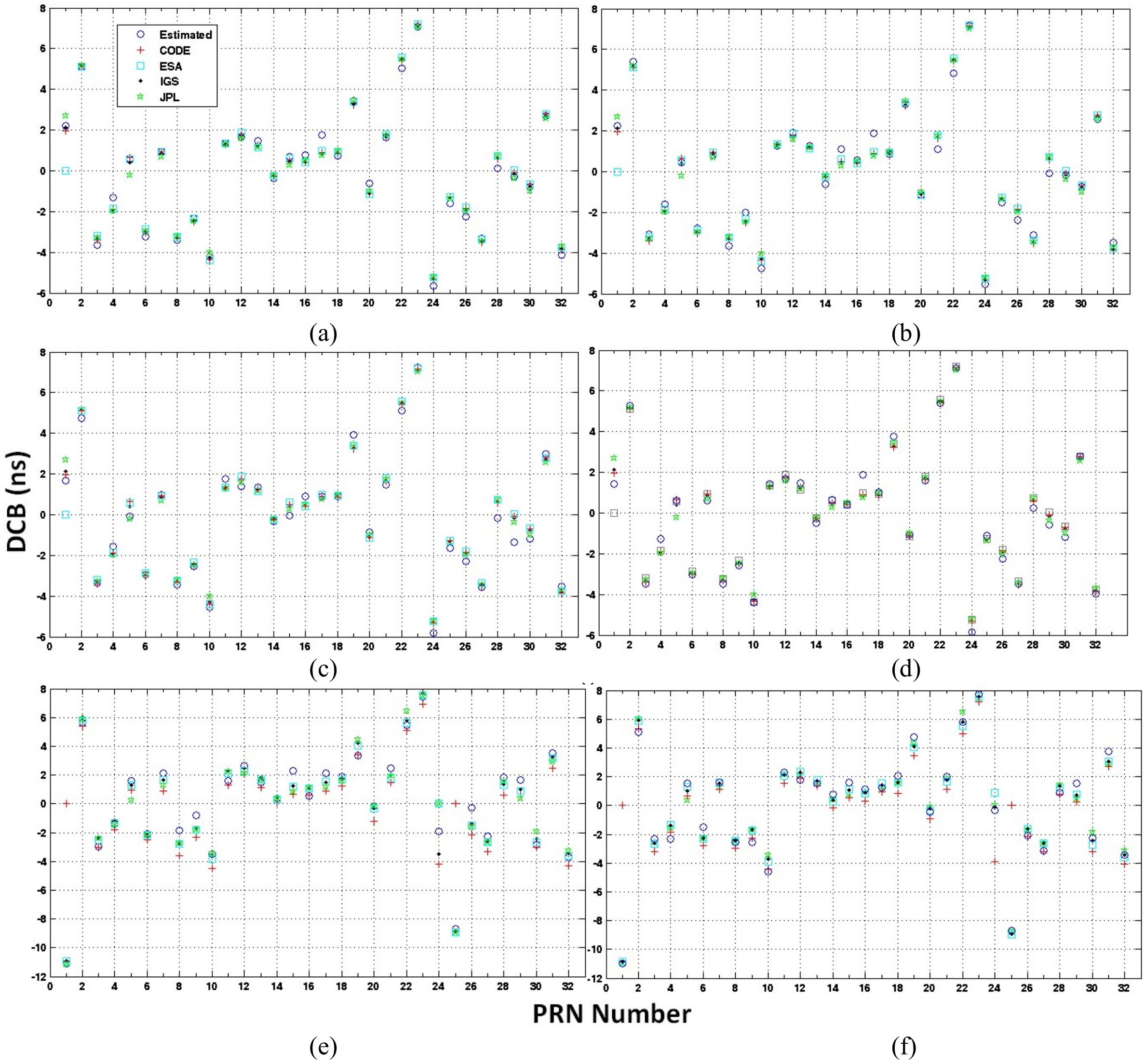

Figure 3. The comparison of the estimated satellite DCB with those estimated by the CODE, ESA, JPL and IGS combined ionosphere maps for (a) Gopi (01-01-2010), (b) Gras (01-01-2010), (c) Pots (01-01-2010), (d) Onsa (01-01-2010), (e) Tehn (15-07-2012), (f) Tehn (07-03-2012).

Second, once the carrier-phase-leveled ionospheric observable was obtained, the corrections for the differential code biases of the satellites and receivers were applied to it. These corrections were obtained from the IONEX files and the proposed method, separately. Figure 5 shows the differences between VTEC values by the estimated satellite and receiver DCBs and VTEC values by the CODE satellite and receiver DCBs. The red-dotted lines represent the accuracy range of the GPS-derived TEC from the carrier to code leveling process method (Dettmering et al., 2011). This figure depicts the meaningful difference between the VTEC estimations from different DCBs and emphasizes the importance of the accurate satellite and receiver DCBs estimations.

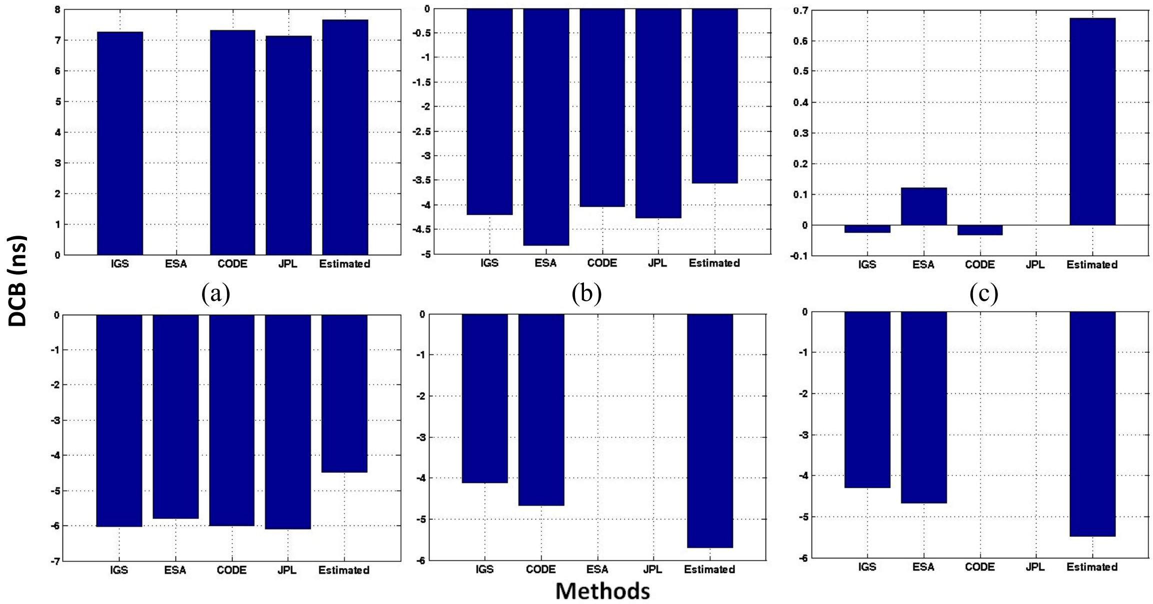

Figure 4. The comparison of the estimated receiver DCB with those estimated by the IGS centers product for (a) Gopi (01-01-2010), (b) Gras (01-01-2010), (c) Pots (01-01-2010), (d) Onsa (01-01-2010), (e) Tehn (15-07-2012), (f) Tehn (07-03-2012).

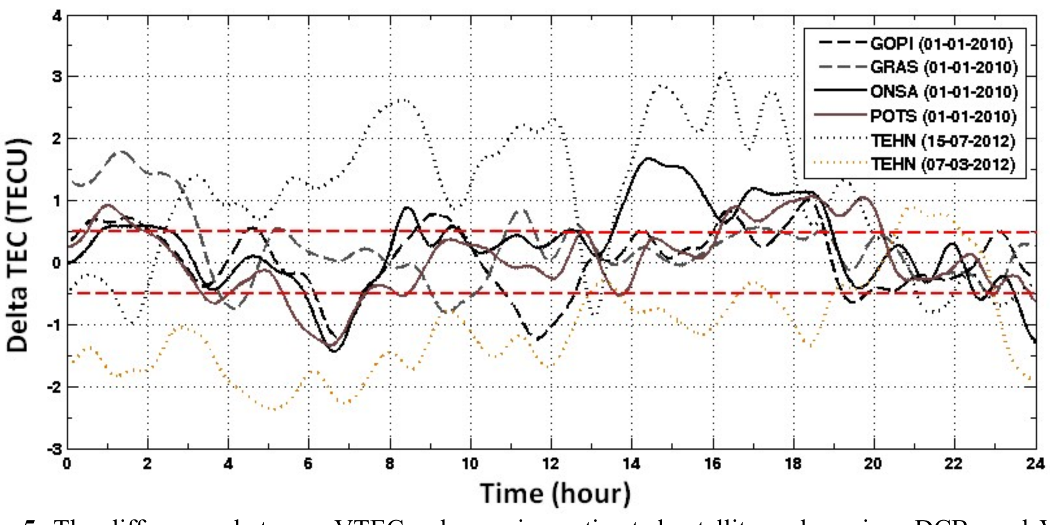

Figure 5. The differences between VTEC values using estimated satellite and receiver DCBs and VTEC values using CODE satellite and receiver DCBs.

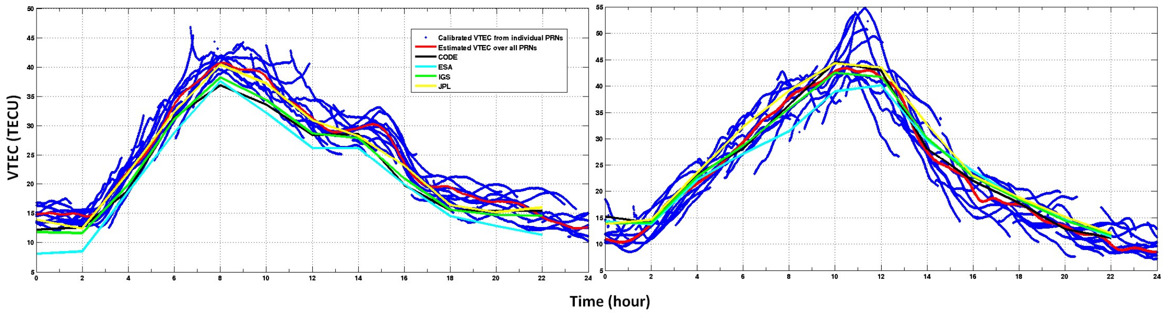

Figure 6. The comparison of the calibrated and estimated VTEC with the estimated value by the IGS centers product for the Tehn station (left): 7 March 2012, (right): 15 July 2012.

Third, the proposed method was compared with the TEC estimates derived from the IGS centers product. Figure 6 shows the comparison of the estimated TEC values with those estimated by the IGS centers product at the Tehn station. The figure indicates the VTEC with the estimated DCBs, along with those from IGS centers.

4 Conclusions

The total electron content in the ionosphere can be easily estimated from the combination of the Global Positioning System (GPS) data. However, the TEC data derived from the GPS measurements lacks certainty because each GPS signal has a hardware-associated bias that seriously affects the accuracy of the ionospheric TEC estimates. In this research, the regional approach by the spherical Slepian function was used to estimate the GPS satellite and receiver DCBs. This method is based on the estimation of the ionospheric models' coefficients and DCBs from the GPS dual-frequency observations by the weighted least-squares method. The results were compared with those from the IGS centers product and showed that the proposed method is capable of delivering stable and comparable bias estimates.

References

Arikan, F., Nayir, H., Sezen, U., and Arikan, O., 2008, Estimation of single station interfrequency receiver bias using GPS-TEC: Radio Science, **43**, RS4004. Doi: 10.1029/2007RS003785

Chen, W., Hu, C., Gao, S., Chen, Y., and Ding, X., 2004, Absolute ionospheric delay estimation based on GPS PPP and GPS active network: International Symposium on GNSS/GPS, Sydney, Australia, 6–8 Dec, 2004.

Ciraolo, L., Azpilicueta, F., Brunini, C., Meza, A., and Radicella, S., 2007, Calibration errors on experimental slant total electron content (TEC) determined with GPS: Journal of Geodesy, **81**, 111–120. Doi: 10.1007/s00190-006-0093-1

Coco, D., Coker, C., Dahlke, S., and Clynch, J., 1991, Variability of GPS satellite differential group delay biases: IEEE Transactions on Aerospace and Electronic Systems., **27**, 931–938.

Conte, J., Azpilicueta, F., and Brunini, C., 2011, Accuracy assessment of the GPS-TEC calibration constants by means of a simulation technique: Journal of Geodesy, **85**, 1–8. Doi: 10.1007/s00190-011-0477-8

Dach, R., Hugentobler, U., Fridez, P., and Meindle, M., 2007, Bernese GPS software version 5.0: Astronomical Institute, University of Bern, Switzerland.

Dettmering, D., Heinkelmann, R., and Schmidt, M., 2011, Systematic differences between VTEC obtained by different space-geodetic techniques during CONT08: Journal of Geodesy, **85**, 443–451.

Durmaz, M., and Karslioglu, M. O., 2014, Regional vertical total electron content (VTEC) modeling together with satellite and receiver differential code biases (DCBs) using semi-parametric multivariate adaptive regression B-splines (SP-BMARS): Journal of Geodesy, **89,** 347–360. Doi: 10.1007/s00190-014-0779-8

Gao, Y., Heroux, P., and Kouba, J., 1994, Estimation of GPS receiver and satellite L1/L2 signal delay biases using data from CACS: Proceedings of the International Symposium on Kinematic Systems in Geodesy, Geomatics and Navigation, 109–117, August 30–September 2, Banff, Canada.

Hofmann-Wellenhof, B., Lichtenegger, H., and Wasle, E., 2008, GNSS – Global Navigation Satellite Systems – GPS, GLONASS, Galileo & more: Springer-Verlag, Wien.

Jakowski, N., Sardon, E., Engler, E., Jungstand, A., and Klahn, D., 1996, Relationships between GPS-signal propagation errors and EISCAT observations: Annals of Geophysics, **14**, 1429–1436.

Jin, S. G., Luo, O. F., and Park, P., 2008, GPS observations of the ionospheric F2-layer behavior during the 20th November 2003 geomagnetic storm over South Korea: Journal of Geodesy, **82,** 883–892. doi:10.1007/ s00190-008-0217-x

Jin, R., Jin, S., and Feng, G., 2012, M_DCB: Matlab code for estimating GNSS satellite and receiver differential code biases: GPS Solutions, **16**, 541–548.

Kee, C., and Yun, D., 2002, Extending coverage of DGPS by considering atmospheric models and corrections: Journal of Navigation, **55**, 305–322. doi:10.1017/S0373463302001741

Komjathy, A., Sparks, L., Wilson, B. D., and Mannucci, A. J., 2005, Automated daily processing of more than 1000 ground-based GPS receivers for studying intense ionospheric storms: Radio Science, **40**, S6006. Doi: 10.1029/2005RS003279

Lanyi, G. E., and Roth, A., 1998, Comparison of mapped and measured total ionospheric electron content using global positioning system and beacon satellite observation: Radio Science, **23**, 483–292.

Lin, L. S., 2001, Remote sensing of ionosphere using GPS measurements: the 22nd Asian Conference on Remote Sensing, 5–9 Nov., Singapore, 2001.

Liu, Z., and Gao, Y., 2003, Ionospheric TEC predictions over a local area GPS reference network: GPS Solutions, **8**, 23–29.

Ma, G., and Maruyama, T., 2003, Derivation of TEC and estimation of instrumental biases from GEONET in Japan: Annals of Geophysics, **21**, 2083–2093.

Mannucci, A. J., Iijima, B. A., Lindqwister, U. J., Pi, X., Sparks, L., and Wilson, B. D., 1999, GPS and ionosphere: Review of Radio Science, 1996–1999: Oxford University Press, New York.

Misra, P., and Enge, P., 2003, Global Positioning System: Signals, Measurements, and Performance: Ganga–Jamuna Press, Massachusetts.

Nohutcu, M., Karslioglu, M. O., and Schmidt, M., 2010, B-spline modeling of VTEC over Turkey using GPS observations: Journal of Atmospheric and Solar-Terrestrial Physics, **72**, 617–624.

Otsuka, Y., Ogawa, T., Saito, A., Tsugawa, T., Fukao, S., and Miyazaki, S., 2002, A new technique for mapping of total electron content using GPS network in Japan: Earth Planets Space, **54**, 63–70.

Ray, J., and Senior, K., 2005, Geodetic techniques for time and frequency comparisons using GPS phase and code measurements: Metrologia **42**, 215–232. doi:10.1088/0026-1394/42/4/005

Schaer, S., 1999, Mapping and predicting the Earth's ionosphere using the Global Positioning System: Ph.D. Thesis, Astronomical Institute, University of Berne, Switzerland.

Schaer, S., Beutler, G., Mervart, L., Rothacher, M., and Wild, U., 1995, Global and regional ionosphere models using the GPS double difference phase observable: In Gendt G., and Dick, G., (Eds.), Proceedings of the IGS Workshop 1995 on Special Topics and New Directions, 15–18 May 1995, GFZ, Potsdam, Germany, pp. 77–92.

Seeber, G., 2003, Satellite Geodesy: Foundations, Methods and Application: Walter de Gruyter, Berlin and New York, 589 pp.

Sharifi, M. A., and Farzaneh, S., 2013, The spatio–spectral localization approach to modelling VTEC over the western part of the USA using GPS observations: Advances in Space Research, **54**, 908–916.

Sharifi, M. A., and Farzaneh, S., 2015, Regional TEC dynamic modeling based on Slepian functions: Advances in Space Research, **56**, 907–915.

Wen, D., Liu, S., and Tang, P., 2010, Tomographic reconstruction of ionospheric electron density based on constrained algebraic reconstruction technique: GPS Solutions, **14**, 375–380. Doi: 10.1007/s10291-010-0161-0

Wielgosz, P., Grejner-Brzezinska, D., and Kashani, I., 2003, Regional ionosphere mapping with kriging and multiquadratic methods: Journal of Global Positioning System: **2**, 48–55.

Wilson, B. D., Mannucci, A. J., 1993, Instrumental biases in ionospheric measurement derived from GPS data: In paper presented at proceedings of the ION GPS-93, Salt Lake City, UT, September 22–24, pp 1343–1351.

Wilson, B. D., Yinger, C. H., Feess, W. A., and Shank, C., 1999, Newand improved: the broadcast interfrequency biases: GPS World, **10,** 56–66.

Yuan, Y., and Ou, J., 1999, The effects of instrumental bias in GPS observations on determining ionospheric delays and the methods of its calibration: Acta Geodaetica et Geophysica. Cartogr. Sin., **2,** 110–114. Doi: cnki:ISSN: 1001-1595.0.1999-02-002

Zhang, Y., Wu, F., Kubo, N., and Yasuda, A., 2003, TEC measurement by single dual-frequency GPS receiver: paper presented at International Symposium on GPS/GNSS, Tokyo, 15–18, Nov, 2003.